Cyclodehydrogenation catalyzed by atomic hydrogen

Authors: Rafal Zuzak,[1] Pawel Dabczynski,[1] Jesús Castro-Esteban,[2&] José Ignacio Martínez,[3] Mads Engelund,[4] Dolores Pérez,[2] Diego Peña,[2*] and Szymon Godlewski[1*]

Affiliations:

[1] Faculty of Physics, Astronomy and Applied Computer Science, Jagiellonian University, PL 30-348 Krakow, Poland

[2] Centro de Investigación en Química Biolóxica e Materiais Moleculares (CiQUS) and Departamento de Química Orgánica, Universidade de Santiago de Compostela, 15782 Santiago de Compostela, Spain;

[3] Instituto de Ciencia de Materiales de Madrid, Consejo Superior de Investigaciones Científicas (ICMM-CSIC), 28049 Madrid, Spain

[4] Espeem S.A.R.L. (espeem.com), L-4206 Esch-sur-Alzette, Luxembourg

*Corresponding author. Email: szymon.godlewski@uj.edu.pl, diego.pena@usc.es

[&]present address: Department of Chemistry, Massachusetts Institute of Technology, 77 Massachusetts Avenue, Cambridge, Massachusetts 02139, United States

Abstract: Atomically precise synthesis of nanographenes and graphene nanoribbons on semiconductors and insulators has been a formidable challenge. In particular, the metallic substrates needed to catalyze cyclodehydrogenative planarization reactions of precursor molecules limit subsequent applications that exploit the electronic structure of nanographenes. We demonstrate that, counterintuitively, atomic hydrogen can play the role of a catalyst in the cyclodehydrogenative planarization reaction regardless of the substrate type. The high efficiency of the method was demonstrated by the nanographene synthesis on metallic Au, semiconducting TiO_2, as well as on inert and insulating Si/SiO_2 and thin NaCl layers.

The diverse structural shapes of nanographenes [1, 2, 3, 4, 5, 6, 7, 8] and graphene nanoribbons (GNRs) [9, 10, 11, 12, 13] can exhibit electronic [14] and magnetic [12, 13] properties that arise from their distinctive electron confinement geometries. Their synthesis has been approached by using solution organic chemistry to deliver molecular precursors that undergo surface-catalyzed inter- and intramolecular transformations under ultrahigh vacuum (UHV) conditions after deposition on the target substrate surface [15]. For example, planarization of a precursor through cyclodehydrogenative C-C coupling yields polycyclic, conjugated graphene-based structures [9]. This crucial step can be reliably and efficiently initiated on noble metal surfaces [9, 15]. However, the high density of metallic substrate electronic states also affects the electronic properties of the product molecule and devices fabricated on such substrates, and has prompted a search for alternative routes [16]. Examples of on-surface synthesis on nonmetallic substrates are relatively scarce [16-30], and the planarization pathways have been limited to individual examples of cyclodehydrogenation [31] or cyclodehydrodefluorination [32, 33] on very specific faces of rutile titania crystal.

We now report a strategy that allows the formation of planar sp^2 carbon-based moieties on a range of substrates. Atomic hydrogen has been used for on-surface synthesis experiments to remove polymerization by-products [34, 35], protect reactive edges [36], induce heteroatom [34] or isotope substitution [37], tailor reactions [38], quench organometallic states [39], hydrogenate GNRs [40] or induce intermolecular fusion [41]. We report dosing of atomic hydrogen to initiate the cyclodehydrogenation reaction of precursors in a manner independent of the substrate (Fig. 1). The approach was verified based on high-resolution scanning tunneling microscopy (STM) imaging, bond-resolved non-contact atomic force microscopy (nc-AFM) visualization [42] and time-of-flight secondary-ion mass spectrometry (ToF-SIMS) measurements with metallic, semiconducting, and insulating substrates. Climbing-Image Nudged-Elastic Band (CI-NEB) calculations were used to explore the reaction path theoretically.

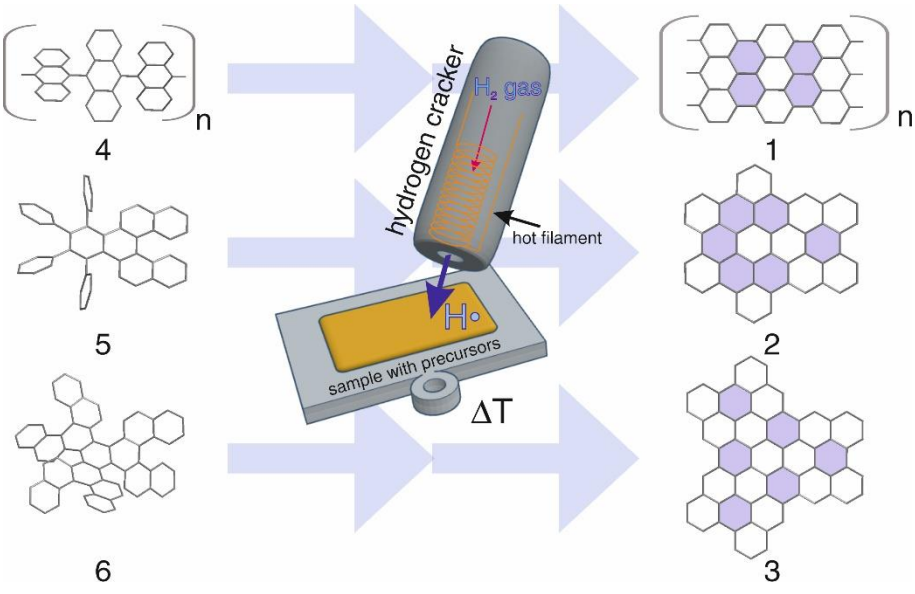

Fig. 1. Cyclodehydrogenation catalyzed by atomic hydrogen. Polymers 4 and flexible precursors 5, 6 are transformed into graphene derivatives 1, 2, 3.

To test this approach, we selected 10,10'-dibromo-9,9'-bianthracene (DBBA) as a precursor of GNRs **1**, and specially designed and synthesized compounds **5** and **6**, as molecular precursors of nanographenes **2** and **3**, respectively. These precursors allowed us to analyze the planarization of both polymeric units in **4**, as well as structures containing phenyl substituents

with free rotation (**5**) and helical moieties whose geometrical orientation is governed by the steric hindrance (**6**).

Planarization through cyclodehydrogenation initiated by atomic hydrogen

We started the experiments with the Au(111) surface, which serves as an example of the metallic substrate, and also allowed for the in-depth analysis of the reaction products by both high- resolution STM and bond-resolved nc-AFM microscopy [42]. Figure 2A shows the typical STM image of 7-armchair graphene nanoribbons (7-AGNRs, **1**) synthesized on Au(111) by dosing of atomic hydrogen. The GNRs are fabricated in a two-step process: (i) (DBBA) was polymerized thermally at 200°C by means of Ullmann-like coupling to obtain polyanthryl **4**, and (ii) these polymers were subjected to atomic hydrogen dosed for 30 minutes at $1 \cdot 10^{-7}$ mbar (molecular hydrogen gas pressure) while keeping the sample at 220°C.

The STM topography showed the presence of mainly defect-free 7-AGNRs (**1**); the two blue arrows indicate the occurrence of incompletely planarized units (Fig .2A). The planarization was very efficient, and in general more than 99% of possible new C-C bonds are formed and associated benzene rings between anthracene units are already created, leaving the non-fully-reacted unfinished GNR structures indicated by arrows as sole examples (for details see SI). During the hydrogen dosing procedure bromine atoms, which are the polymerization reaction by-products, were removed from the surface [34] as HBr molecules [43].

In our experiment, the sample temperature during dosing was selected to ensure efficiency of the cyclodehydrogenation process (see SI Fig. S3 for details). The generation of 7-AGNRs presented here was achieved at 220°C, well below the temperature range (> 320°C) at which the catalytic activity of Au(111) promotes cyclodehydrogenation [9,15]. This lower temperature suggested that a different reaction pathway was initiated by dosing with atomic hydrogen, which could be examined by closer examination of the GNR structures. In Fig. 2B, we distinguished different terminations at both ends of the GNR, which is caused by the attachment of two hydrogen atoms at the center of one termini and formation of a sp^3 carbon methylene moiety ($-CH_2-$), as visualized by bond-resolved nc-AFM images supplemented by high-resolution STM topographies in Fig. 2, C to F. The difference in appearance of the two termini in high resolution STM pictures was caused by the methylene unit, which quenched the radical character associated with the zig-zag termination [44-45].

This presence of either perfect zig-zag or methylene bridged (previously named as superhydrogenated [41]) edges enabled unambiguous identification of the reaction products. Crucially, the nc-AFM images of arm-chair sides of the GNRs (Fig. 2, D and F) did not show the features associated with formation of methylene moieties and had perfect flat edge termination. The STM appearance of superhydrogenated zig-zag edges (Fig. 2, B and E) is in accordance with previous reports [45] and suggest that unwanted additional hydrogen atoms were removed after annealing at 300°C [36]. In our experiment, we estimate the abundance of superhydrogenated zig-zag edges at approximately 66% (158 out of 240 counted zig-zag termini), and that after annealing to 300 °C, the fraction of methylene units was reduced to < 1% leaving almost exclusively perfectly shaped and terminated 7-AGNRs based on sp^2 carbon atoms.

In order to demonstrate the versatility of the approach, we used hydrogen-assisted planarization to form nanographenes **2**. The bond-resolved nc-AFM (Fig. 2G, inset) shows the atomic structure of **2** generated with atomic hydrogen at 220°C. We note that the synthesis of nanoflakes **2** by purely thermal means cannot be achieved < 300°C, and that the perfect shaping of the edges indicates that no additional hydrogen atoms (methylene moieties) were present. Additionally, in the temperature range of our hydrogenation experiments (up to 220°C), we did

not observe any signs of intermolecular cross-coupling as reported for molecules activated with higher pressure of atomic hydrogen [41].

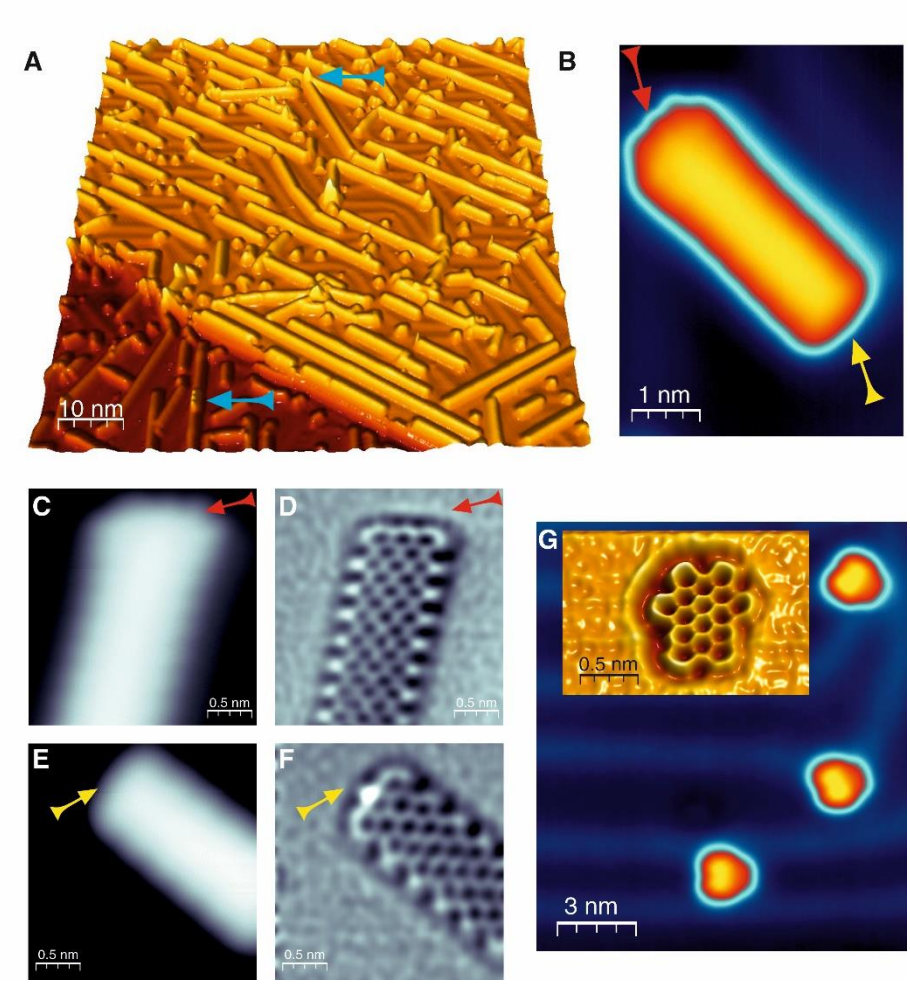

Fig. 2. Cyclodehydrogenation promoted by atomic hydrogen at 220°C on Au(111). (A) 3D STM image with 7-AGNRs (**1**), blue arrows indicate rarely observed incompletely planarized DBBA units; (B) filled state STM image of the 7-AGNR (**1**) with differently terminated zig-zag edges; high resolution STM (C) and bond-resolved AFM (D) images of perfectly shaped 7-AGNR (**1**) with zig-zag termini indicated by red arrows; STM (E) and nc-AFM (F) images of 7-AGNR (**1**) with methylene (sp^3 carbon) bridged end indicated by yellow arrows; (G) high resolution STM image of nanographenes **2**, inset shows bond-resolved AFM image visualizing perfect shaping of **2**; tunneling current: 50 pA (A), 25 pA (B, C, E, and G), bias voltage: -1 V.

We replaced the metallic substrate with a semiconductor surface, TiO_2(110) – (1x1), which allowed us to compare directly with the recently reported thermally initiated cyclodehydrogenation that occurs at 400°C [31]. We analyzed the ability to efficiently initiate cyclodehydrogenation with atomic hydrogen both between vicinal phenyl rings rotating around σ bonds in **5** as well as within strained pentahelicenes of **6**. The generated target nanographenes **2** and **3**, respectively, were shown in Fig. 3. Compounds **2** and **3** could be discerned in the high resolution STM images acquired at voltages corresponding to the molecule gap visualized in Fig. 3, A and F.

In order to unambiguously demonstrate planarization of both precursors **5** and **6**, STM imaging with voltages adjusted to the energy levels of **2** and **3** molecular states were acquired following the spectroscopic (STS) characterization in reference [31]. Our interpretation of these measurements is corroborated by theoretical image simulations [46], in which voltage was

assumed to activate the HOMO/LUMO (highest occupied molecular orbital/lowest unoccupied molecular orbital) state of the gas phase molecule. The comparison is displayed in Fig. 3, B to E and Fig. 3, G to J, for **2** and **3**, respectively. Very strong agreement between calculations and experiment confirmed the synthesis of the expected molecules, and the strong match with gas-phase calculations suggested a limited interaction of nanoflakes **2** and **3** with TiO_2(110)-(1x1) in accordance with our previous findings for thermally planarized compounds [31].

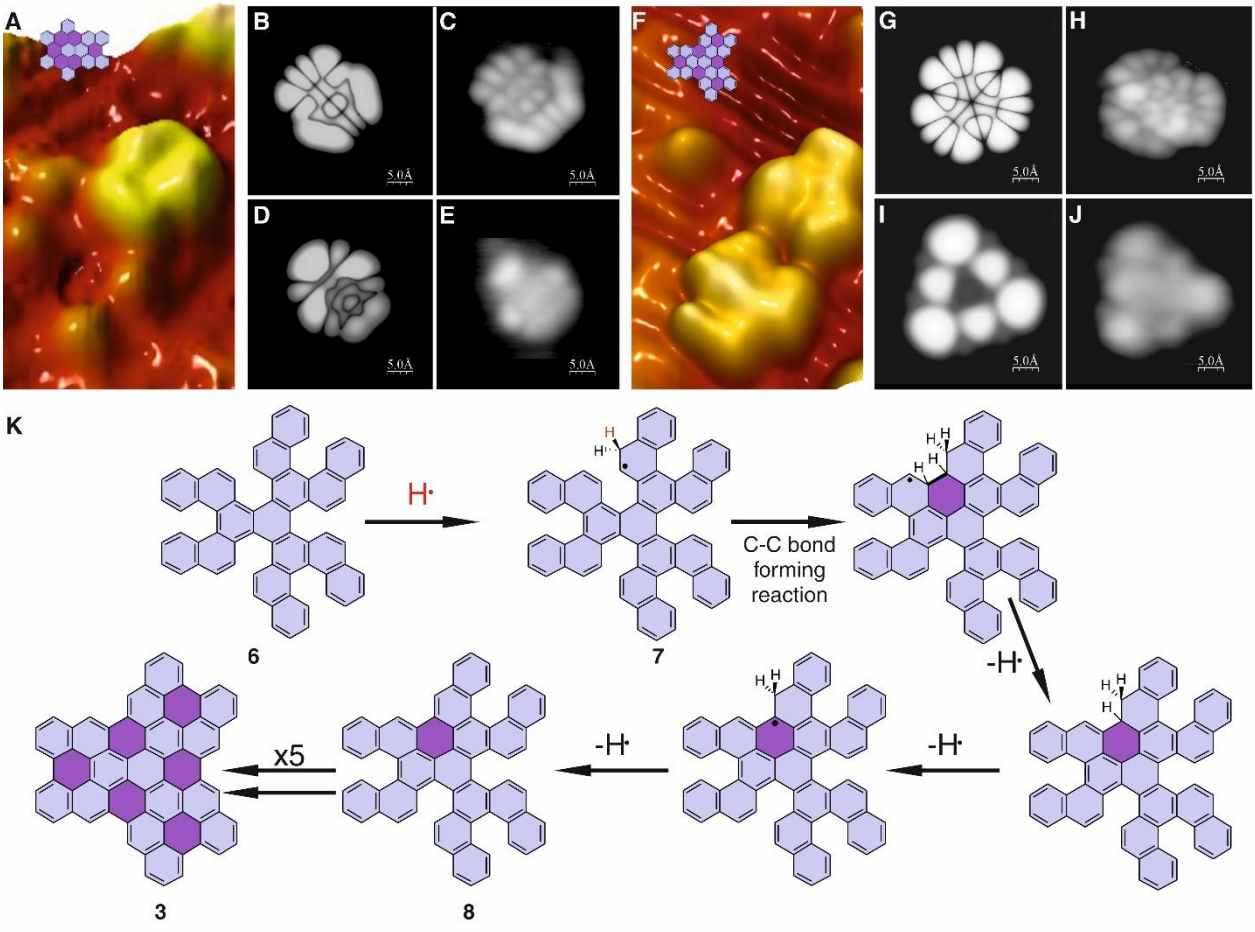

Fig. 3. Atomic hydrogen induced planarization yielding nanographenes 2 and 3 on TiO_2(110)-(1x1). (A) 3D STM view of nanographenes 2; high-resolution simulated (B) and experimental (C) filled-state images of **2**; high-resolution simulated (D) and experimental (E) empty state images of **2**; (F) 3D STM image of nanographene **3**; high resolution simulated (G) and experimental (H) filled state images of **3**; high-resolution simulated (I) and experimental (J) empty state images of **3**; (K) plausible reaction mechanism for planarization of **6** into **3** catalyzed by atomic hydrogen; bias voltage: +1.5 V (A and F), -1.7 V (C), +2.3 V (E), -1.5 V (H), +2.2 V (J); tunneling current: 10 pA (C and J), 15 pA (A, E, F, and H).

The efficient cyclodehydrogenation initiated under similar conditions on both Au(111) and TiO_2(110)-(1x1) suggested that, in our experiments, the externally dosed atomic hydrogen, not the substrate, catalyzed the reaction, which may seem counterintuitive given that atomic hydrogen dosing facilitated the removal of covalently-bonded hydrogen. Figure 3K shows a mechanistic proposal for the conversion of **6** into **3**, which is inspired by Sánchez-Sánchez and co-workers reporting on-surface hydrogen-induced covalent coupling of polycyclic aromatic hydrocarbons [41]. Atomic hydrogen likely added to compound **6** to form various π radicals. If this radical was placed in the fjord region of a pentahelicene moiety (for example, **7**), it would continue to react to form an intramolecular C-C bond, followed by a sequence of C-H cleavage

reactions to obtain structure **8**. Similar transformations in the other fjord regions of the intermediate molecules would lead to the flat nanographene **3**.

In order to validate the mechanistic proposal (Fig. 3K) we have performed a comprehensive series of theoretical atomistic simulations using pentahelicene as a proof-of-concept model system for the cyclodehydrogenation reaction. The pentahelicene unit could be regarded as a representative of the molecular fjord region involved in the sequential cyclodehydrogenative planarization of compound **6**. The calculated mechanism progression involves: (i) atomic H addition to the peripheral C atom forming a π-radical (energy barrier: 0.08 eV), which activates the molecule for (ii) cyclization through C-C coupling generating the new six-membered ring (energy barrier: 0.56 eV). Subsequently, we propose (iii) three consecutive Eley-Rideal hydrogen abstraction reactions [47] forming three gas-phase H_2 molecules (maximum energy barrier of 0.01 eV), which lead to the full planarization of the molecular structure. All intermediate sub-reactions exhibit net free energy gains ranging from -0.5 to -3.3 eV. Therefore, the aforementioned C-C bond formation is the limiting reaction step, featuring a moderate energy barrier of 0.56 eV making the process highly probable in the experimentally applied temperature range (for details see SI Fig. S4).

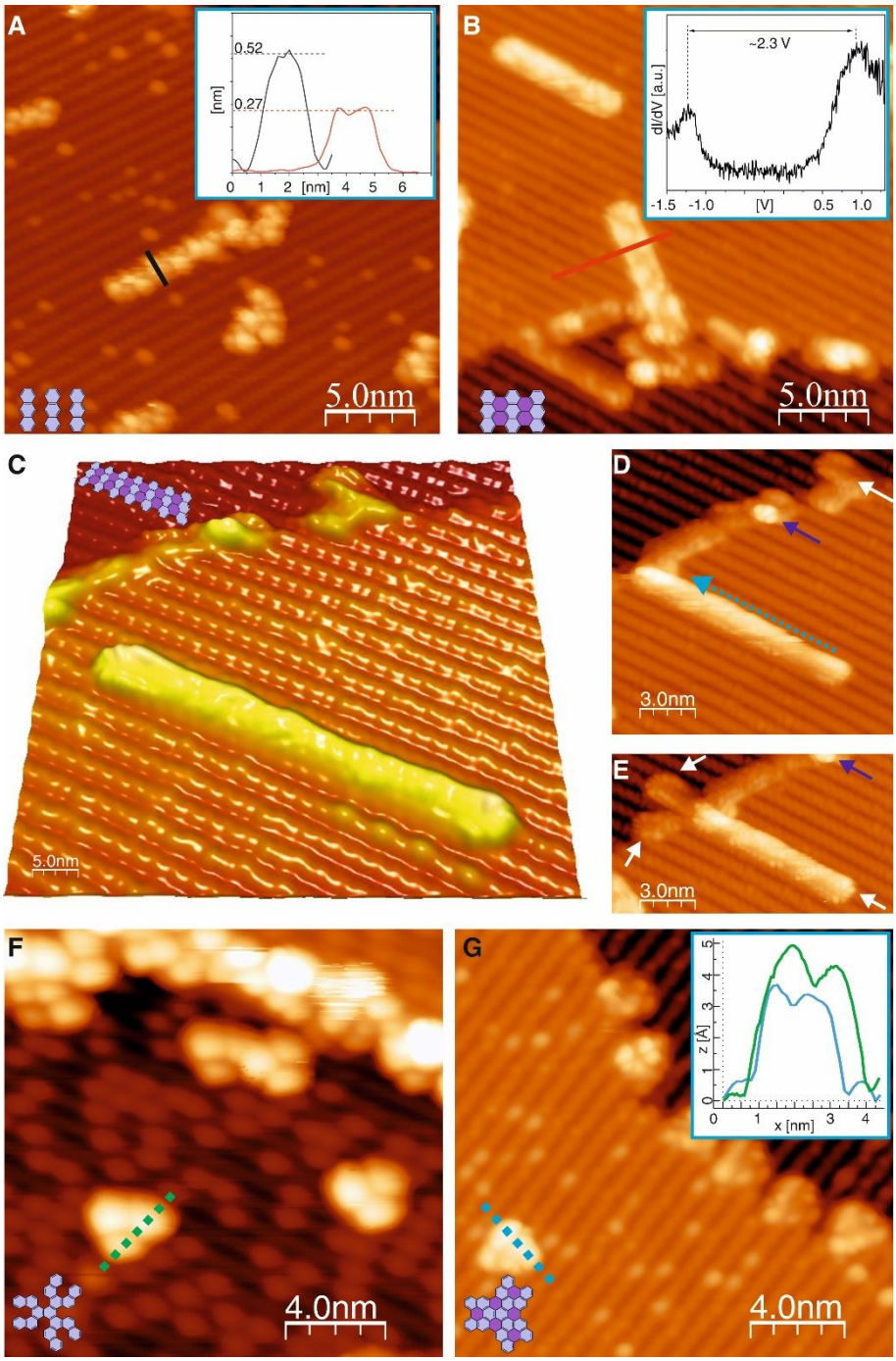

Fig. 4. 7-AGNRs (1) and nanographenes 3 synthesized on TiO_2(011)-(2x1) by atomic hydrogen induced cyclodehydrogenation. Typical STM images of DBBA based polymers 4 (A) and 7-AGNRs **1** (B) after atomic hydrogen treatment, inset in (A) shows easily discernible apparent height difference between DBBA-based polymers and 7-AGNRs, inset in (B) shows occurrence of electronic states associated with zig-zag end of 7-AGNR; (C) 3D visualization of long 7-AGNR oriented along the surface reconstruction rows; (D) lateral manipulation of 7-AGNR, light blue arrow indicates direction of GNR movement, dark blue arrow indicates a defect playing a role of a position marker; (E) 7-AGNR manipulated over the surface step edge, white arrows indicate clearly discernible characteristic appearance of the GNR termini; (F) STM image of precursors **6** (F) and nanographenes **3** (G), the inset in G indicates the noticeable difference of the apparent height of **6** and **3**; tunneling current: 5 pA (A), 10 pA (F), 15 pA (B, C, and G), 100 pA (D and E), bias voltage: +1.5 V (A through F), +2.3 V (G).

The above described route should enable the generation of nanoflakes and GNRs on surfaces that do not catalyze these reactions. To demonstrate this possibility, we used TiO_2(011)-(2x1), which promotes Ullmann-like polymerization [17-18] but cannot be used for thermally-driven cyclodehydrogenation [32, 33]. Figure 4 demonstrates the successful synthesis of 7-AGNRs (**1**) from standard DBBA precursors through a two-step process: (i) intermolecular thermally driven (260°C) polymerization yielding DBBA-based polymers **4** [17] (Fig. 4A) followed by (ii) hydrogen-initiated cyclodehydrogenation (atomic hydrogen, 220°C) to afford 7-AGNRs (Fig. 4B). The successful planarization was supported by the apparent height comparison of the polymers and GNRs (green and red curves in the inset of Fig. 4A, respectively), as well as by the STS characterization of the electronic end states associated with zig-zag termini of GNRs displayed in the inset of Fig. 4B. The STS results were in good agreement with previous reports for 7-AGNRs generated through the cyclodehydrodefluorination from specially designed molecular precursors [33].

Furthermore, our approach delivered not only GNRs immobilized by surface steps or domain boundaries, but also mobile ones that usually aligned with the reconstruction rows of the substrate. An example of a mobile GNR is presented in 3D mode in Fig. 4C supplemented by the demonstration of the tip-induced manipulation (Fig. 4D) that led to the GNRs displacement over the surface step edge imaged in Fig. 4E. Notably, the ends of the GNR were clearly identified by the characteristic features originating from the distinct electronic states associated with the zig-zag edge [33]. The demonstration of the successful planarization induced by atomic hydrogen (220°C) was further extended to the synthesis of nanographenes **3** from nonplanar starting material **6,** as shown by high-resolution STM images in Fig. 4, F and G, as well as the closed layer of **3** (Fig. S5). Importantly, nanographenes **3** have not been synthesized on TiO_2(011)-(2x1) by thermal treatment without the application of atomic hydrogen.

Nanographenes synthesized directly on insulators

Synthesizing graphene materials on insulating surfaces is more challenging because of the lower interaction energy between the precursor and the substrate compared to metals and semiconductors, which may promote desorption rather than cyclodehydrogenation. In addition, the atomic-scale characterization of reaction products is also challenging because STM cannot be used on insulating surfaces. The hydrogen-induced planarization reaches high efficiency between 200° and 220°C, and at these temperature internal cyclodehydrogenation may compete with desorption. Indeed, we observed the thermal desorption of precursor **5**. However, precursor **6** showed stronger interaction with the substrate because of its size and shape, which facilitated the formation (through cyclodehydrogenation) of the planarized nanographene **3**.

We used the silicon covered with ~ 300 nm of silicon dioxide (SiO_2) as a substrate to demonstrate on-surface synthesis of nanographenes on insulators (Fig. 5A). This interface is widely applied in electronics industry [48], and it has also attracted attention as a basic substrate for fabrication of low-dimensional devices [49, 50]. Importantly, the top SiO_2 layer is not only resistant to atomic hydrogen, but the exposure at 200°C to 300°C may even improve surface quality [51, 52]. To demonstrate the versatility of the approach we have performed additionally similar experiments yielding nanoflakes **3** on two additional insulators: bulk NaCl (Fig. S7, S8) and thin salt layer on copper NaCl/Cu(111) (Fig. S6).

In order to monitor the transformation from precursor **6** into planar nanographene **3**, we applied ToF-SIMS [37, 53-54]. Figure 5B presents the mass spectra for **6** deposited on Si/SiO_2 plotted in red that showed the presence of precursors **6** by a series of peaks at 828 to 830 Da that reflected the natural abundance of carbon isotopes. Additional peaks recorded at masses starting from 816 up to 827 Da we could attribute to the precursors in various states of dehydrogenation induced by ToF-SIMS measurements [53]. The tail extended exactly to the fully

dehydrogenated nanographene **3** in accordance with the previous report on a metallic substrate [53].

The blue curve represents data acquired for the precursors **6** at Si/SiO_2 annealed to 190°C. ToF-SIMS experiments yielded similar results and demonstrated that annealing alone was insufficient to induce transformation from **6** into target compound **3**. In contrast, the green plotted curve shows data acquired for the sample with **6** after treatment with atomic hydrogen at 190°C with clearly discernible nanographenes **3** represented by the series of peaks starting at the mass of 816 Da, thus demonstrating the successfully achieved cyclodehydrogenation on an insulating sample. However, the presence of peaks for masses corresponding to the precursors indicate the presence of unreacted **6** on the surface.

In order to understand the interaction of **3** and **6** on Si/SiO_2, we have performed static ToF-SIMS measurements as a function of the substrate temperature (Fig. 5C). For temperatures > 210°C, the unreacted precursor **6** was almost completely desorbed, whereas generated nanoflakes **3** were still adsorbed on the surface. These nanoflakes **3** were synthesized from **6** by atomic hydrogen produced during ToF-SIMS measurements (for details see Fig. S2). In Fig. 5D, we show the ToF-SIMS data integrated up to 210°C that illustrate the presence of precursors **6**. Fig. 5E shows the ToF-SIMS signal integrated from 210° to 400°C, which indicates the presence of almost exclusively nanoflakes **3** > 210°C.

These results suggested how to prepare a Si/SiO_2 surface covered only with nanoflakes **3**. We prepared the Si/SiO_2 with precursors **6**, which were then treated with atomic hydrogen flux at 190°C, and then annealed at 240°C in order to remove unreacted precursors. The resulting ToF-SIMS data are shown in Fig. 5B on top by a black curve that indicated the presence of nanoflakes **3** with strongly suppressed peaks for the precursor **6**. In the experiments with Si/SiO_2 we took advantage of the robustness of both precursors **6** and nanoflakes **3** and transported the samples from the preparation chamber to the SIMS setup in ambient conditions, whereas controlled experiments with the sample transported in UHV showed no differences.

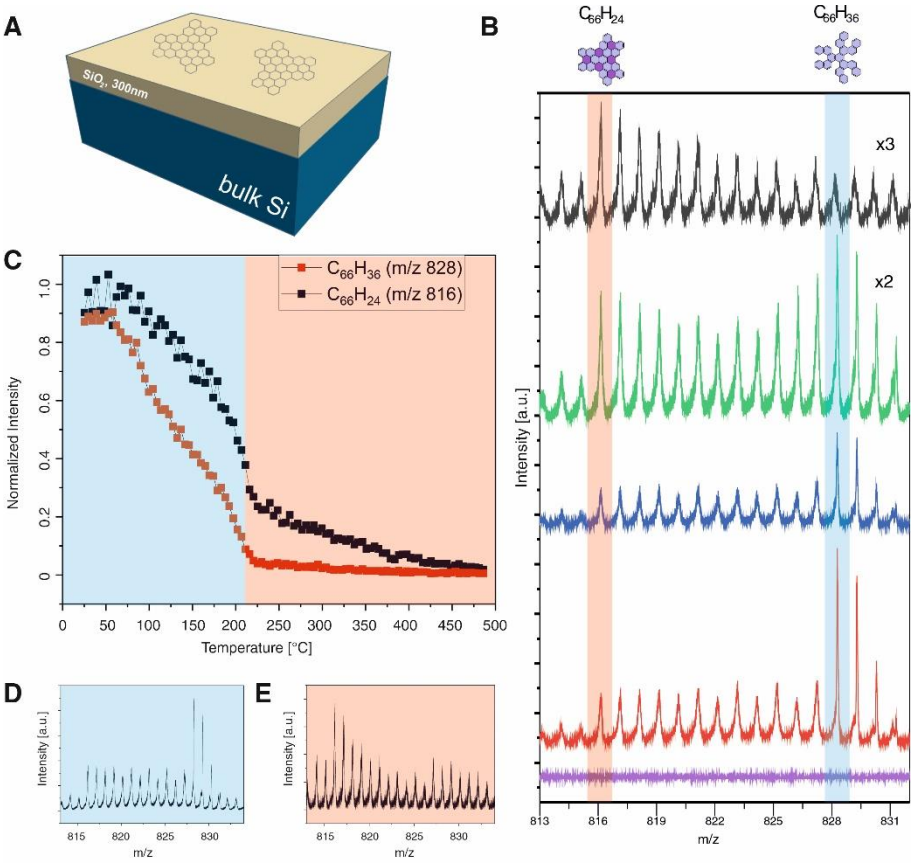

Fig. 5. Synthesis of nanographenes 3 on Si/SiO_2 interface induced by atomic hydrogen. (A) schematic view, (B) ToF-SIMS spectra with $C_{66}H_{24}$ (nanographene **3**) and $C_{66}H_{36}$ (precursor **6**) mass regions marked by transparent red and blue, respectively; colored spectra: violet – reference obtained for clean Si/SiO_2, red –precursors **6** deposited on Si/SiO_2, blue – precursors **6** on Si/SiO_2 after annealing at 190°C, green – mixture of precursors **6** and nanographenes **3** on Si/SiO_2, after annealing at 190°C with atomic hydrogen, black – nanographenes **3** present on the surface after atomic hydrogen treatment at 190°C and subsequent annealing at 240°C; (C) static ToF-SIMS performed on a Si/SiO_2 sample containing precursors **6** showing $C_{66}H_{36}$ (precursor **6**, mass 828.286 Da – red) and $C_{66}H_{24}$ (mass 816.134 Da – black) signals displayed as a function of temperature; (D) mass spectra from (C) integrated from room temperature up to 210°C showing presence of precursors **6**; (E) mass spectra from (C) integrated from 210°C up to 400°C indicating presence of nanoflakes **3**; in (C) data point – to – point normalized to the reference experiment conducted with same primary ion dose density at room temperature.

Conclusions

Transferring the role of the catalyst for the planarization of graphene-like structures from a substrate to the dosage of atomic hydrogen expands the possibilities for constructing nanoscale structures from organic precursors. In particular, the proposed approach may be applied in the development of bulk and low dimensional functional devices combined with graphene-like moieties. In a wider perspective, our research showing the non-intuitive use of atomic hydrogen for cyclodehydrogenation could be extended to explore the possibility of creating non-benzenoid and doped rings, which introduce the desired modifications of electronic properties in the synthesized nanostructures. This approach opens up a design space for molecular electronics by avoiding the limitations posed by electronically disruptive substrates for catalyzing the desired molecular synthesis.

References and Notes

1. M. Treier, C.A. Pignedoli, T. Laino, R. Rieger, K. Müllen, D. Passerone, R. Fasel, Surface-assisted cyclodehydrogenation provides a synthetic route towards easily processable and chemically tailored nanographenes. *Nat. Chem.* **3**, 61-67 (2011).
2. R. Zuzak, I. Pozo, M. Engelund, A. Garcia-Lekue, M. Vilas-Varela, J.M. Alonso, M. Szymonski, E. Guitián, D. Pérez, S. Godlewski, D. Peña, Synthesis and reactivity of a trigonal porous nanographene on a gold surface. *Chem. Sci.* **10**, 10143−10148 (2019).
3. R. Zuzak, J. Castro-Esteban, P. Brandimarte, M. Engelund, A. Cobas, P. Piątkowski, M. Kolmer, D. Pérez, E. Guitián, M. Szymonski, D. Sánchez-Portal, S. Godlewski, D. Peña, Building a 22-ring nanographene by combining in-solution and on-surface syntheses. *Chem. Commun.* **54**, 10256−10259 (2018).
4. S. Mishra, D. Beyer, K. Eimre, S. Kezilebieke, R. Berger, O. Gröning, C.A. Pignedoli, K. Müllen, P. Liljeroth, P. Ruffieux, X. Feng, R. Fasel, Topological frustration induces unconventional magnetism in a nanographene. *Nat. Nanotechnol.* **15**, 22−28 (2020).
5. J. Li, S. Sanz, J. Castro-Esteban, M. Vilas-Varela, N. Friedrich, T. Frederiksen, D. Peña, J.I. Pascual, Uncovering the Triplet Ground State of Triangular Graphene Nanoflakes Engineered with Atomic Precision on a Metal Surface. *Phys. Rev. Lett.* **124**, 177201 (2020).
6. S. Mishra, D. Beyer, K. Eimre, J. Liu, R. Berger, O. Gröning, C. A. Pignedoli, K. Müllen, R. Fasel, X. Feng, P. Ruffieux, Synthesis and Characterization of π-Extended Triangulene. *J. Am. Chem. Soc.* **141**, 10621-10625 (2019).
7. A. Haags, A. Reichmann, Q.T. Fan, L. Egger, H. Kirschner, T. Naumann, S. Werner, J. Sundermeyer, L. Eschmann, F.C. Bocquet, G. Koller, A. Gottwald, M. Richter, M.G. Ramsey, M. Rohlfing, P. Puschnig, J.M. Gottfried, S. Soubatch, F.S. Tautz, Kekulene: On-Surface Synthesis, Orbital Structure, and Aromatic Stabilization. *ACS Nano* **14**, 15766-15775 (2020).
8. J. Hieulle, E. Carbonell-Sanromà, M. Vilas-Varela, A. Garcia- Lekue, E. Guitián, D. Peña, J.I. Pascual, On-surface route for producing planar nanographenes with azulene moieties. *Nano Lett.* **18**, 418−423 (2018).
9. J. Cai, P. Ruffieux, R. Jaafar, M. Bieri, T. Braun, S. Blankenburg, M. Muoth, A.P. Seitsonen, M. Saleh, X. Feng, K. Müllen, R. Fasel, Atomically precise bottom-up fabrication of graphene nanoribbons. *Nature* **466**, 470−473 (2010).
10. P. Ruffieux, S. Wang, B. Yang, C. Sánchez-Sánchez, J. Liu, T. Dienel, L. Talirz, P. Shinde, C. A. Pignedoli, D. Passerone, T. Dumslaff, X. Feng, K. Müllen, R. Fasel, On-surface synthesis of graphene nanoribbons with zigzag edge topology. *Nature* **531**, 489 (2016).
11. S. Kawai, S. Saito, S. Osumi, S. Yamaguchi, A.S. Foster, P. Spijker, E. Meyer, Atomically controlled substitutional boron-doping of graphene nanoribbons. *Nat. Commun.* **6**, 8098 (2015).
12. D.J. Rizzo, G. Veber, T. Cao, C. Bronner, T. Chen, F. Zhao, H. Rodriguez, S.G. Louie, M.F. Crommie, F.R. Fischer, Topological band engineering of graphene nanoribbons. *Nature* **560**, 204–208 (2018).
13. O. Gröning, S. Wang, X. Yao, C. A. Pignedoli, G. Borin Barin, C. Daniels, A. Cupo, V. Meunier, X. Feng, A. Narita, K. Müllen, P. Ruffieux, R. Fasel, Engineering of robust topological quantum phases in graphene nanoribbons. *Nature* **560**, 209–213 (2018).

14. Q.T. Fan, L.H. Yan, M.W. Tripp, O. Krejči, S. Dimosthenous, S.R. Kachel, M.Y. Chen, A.S. Foster, U. Koert, P. Liljeroth, J.M. Gottfried, Biphenylene network: A nonbenzenoid carbon allotrope. *Science* **372**, 852-856 (2021).

15. S. Clair, D.G. de Oteyza, Controlling a Chemical Coupling Reaction on a Surface: Tools and Strategies for On-Surface Synthesis. *Chem. Rev.* **119**, 7, 4717–477 (2019).

16. K. Sun, Y. Fang, L. Chi, On-Surface Synthesis on Nonmetallic Substrates. *ACS Mater. Lett.* **3**, 56−63 (2021).

17. M. Kolmer, A.A. Ahmad Zebari, J.S. Prauzner-Bechcicki, W. Piskorz, F. Zasada, S. Godlewski, B. Such, Z. Sojka, M. Szymonski, Polymerization of Polyanthrylene on a Titanium Dioxide (011)-(2×1) Surface. *Angew. Chem. Int. Ed.* **52**, 10300−10303 (2013).

18. M. Kolmer, R. Zuzak, A.A. Ahmad Zebari, S. Godlewski, J.S Prauzner-Bechcicki, W. Piskorz, F. Zasada, Z. Sojka, D. Bléger, S. Hecht, M. Szymonski, On-surface polymerization on a semiconducting oxide: aryl halide coupling controlled by surface hydroxyl groups on rutile TiO_2(011). *Chem. Commun.* **51**, 11276−11279 (2015).

19. G. Vasseur, M. Abadia, L.A. Miccio, J. Brede, A. Garcia-Lekue, D.G. de Oteyza, C. Rogero, J. Lobo-Checa, J.E. Ortega, Π Band Dispersion along Conjugated Organic Nanowires Synthesized on a Metal Oxide Semiconductor. *J. Am. Chem. Soc.* **138**, 5685−5692 (2016).

20. M. Abadia, G. Vasseur, M. Kolmer, L. Zajac, A. Verdini, J.E. Ortega, L. Floreano, C. Rogero, J. Brede, Increase of Polymerization Yield on Titania by Surface Reduction. *J. Phys. Chem. C* **124**, 16918−16925 (2020).

21. F. Para, F. Bocquet, L. Nony, C. Loppacher, M. Féron, F. Cherioux, D.Z. Gao, F.F. Canova, M.B. Watkins, Micrometre-long covalent organic fibres by photoinitiated chain-growth radical polymerization on an alkali-halide surface. *Nat. Chem.* **10**, 1112−1117 (2018).

22. C.-A. Palma, K. Diller, R. Berger, A. Welle, J. Björk, J.L. Cabellos, D.J. Mowbray, A.C. Papageorgiou, N.P. Ivleva, S. Matich, E. Margapoti, R. Niessner, B. Menges, J. Reichert, X. Feng, H.J. Räder, R.A. Klappenberger, K. Müllen, J.V. Barth, Photoinduced C–C Reactions on Insulators toward Photolithography of Graphene Nanoarchitectures. *J. Am. Chem. Soc.* **136**, 4651− 4658 (2014).

23. M.V. Makarova, Y. Okawa, E. Verveniotis, K. Watanabe, T. Taniguchi, C. Joachim, M. Aono, Self-assembled diacetylene molecular wire polymerization on an insulating hexagonal boron nitride (0001) surface. *Nanotechnology* **27**, 395303 (2016).

24. M. Kittelmann, P. Rahe, M. Nimmrich, C.M. Hauke, A. Gourdon, A. Kühnle, On-Surface Covalent Linking of Organic Building Blocks on a Bulk Insulator. *ACS Nano* **5**, 8420−8425 (2011).

25. A. Richter, V. Haapasilta, C. Venturini, R. Bechstein, A. Gourdon, A.S. Foster, A. Kühnle, Diacetylene polymerization on a bulk insulator surface. *Phys. Chem. Chem. Phys.* **19**, 15172− 15176 (2017).

26. A. Kutz, M.T. Rahman, V. Haapasilta, C. Venturini, R. Bechstein, A. Gourdon, A.M. Foster, A. Kühnle, Impact of the reaction pathway on the final product in on-surface synthesis. *Phys. Chem. Chem. Phys.* **22**, 6109−6114 (2020).

27. A. Richter, M. Vilas-Varela, D. Peña, R. Bechstein, A. Kühnle, Homocoupling of terminal alkynes on calcite (10.4). *Surf. Sci.* **678**, 106−111 (2018).

28. M. Kittelmann, M. Nimmrich, R. Lindner, A. Gourdon, A. Kühnle, Sequential and Site-Specific On-Surface Synthesis on a Bulk Insulator. *ACS Nano* **7**, 5614−5620 (2013).

29. A. Richter, A. Floris, R. Bechstein, L. Kantorovich, A. Kühnle, On-surface synthesis on a bulk insulator surface. *J. Phys.: Condens. Matter* **30**, 133001 (2018).

30. M. Lackinger, Synthesis on inert surfaces. *Dalton Trans.* **50**, 10020 (2021).

31. R. Zuzak, J. Castro-Esteban, M. Engelund, D. Pérez, D. Peña, S. Godlewski, On-Surface Synthesis of Nanographenes and Graphene Nanoribbons on Titanium Dioxide. *ACS Nano* **17**, 2580−2587 (2023).

32. M. Kolmer, R. Zuzak, A.K. Steiner, L. Zajac, M. Engelund, S. Godlewski, M. Szymonski, K. Amsharov, Fluorine-programmed nanozipping to tailored nanographenes on rutile TiO_2 surfaces. *Science* **363**, 57−60 (2019).

33. M. Kolmer, A.K. Steiner, I. Izydorczyk, W. Ko, M. Engelund, M. Szymonski, A.-P. Li, K. Amsharov, Rational synthesis of atomically precise graphene nanoribbons directly on metal oxide surfaces. *Science* **369**, 571−575 (2020).

34. R. Zuzak, A. Jančařík, A. Gourdon, M. Szymonski, S. Godlewski, On-Surface Synthesis with Atomic Hydrogen. *ACS Nano* **14**, 13316-13323 (2020).

35. M. Abyazisani, J.M. MacLeod, J. Lipton-Duffin, Cleaning up after the Party: Removing the Byproducts of On-Surface Ullmann Coupling. *ACS Nano* **13**, 9270– 9278 (2019).

36. J. Lawrence, A. Berdonces-Layunta, S. Edalatmanesh, J. Castro-Esteban, T. Wang, A. Jimenez-Martin, B. de la Torre, R. Castrillo-Bodero, P. Angulo-Portugal, M.S.G. Mohammed, A. Matěj, M. Vilas-Varela, F. Schiller, M. Corso, P. Jelinek, D. Peña, D.G. de Oteyza, Circumventing the stability problems of graphene nanoribbon zigzag edges. *Nat. Chem.* **14**, 1451-1458 (2022).

37. Ch. Wäckerlin, On-Surface Hydrogen/Deuterium Isotope Exchange in Polycyclic Aromatic Hydrocarbons. *Angew. Chem. Int. Ed.* **60**, 8446–8449 (2021).

38. Z.A. Enderson, H. Murali, R.R. Dasari, Q. Dai, H. Li, T.C. Parker, J.-L. Brédas, S.R. Marder, P.N. First, Tailoring On-Surface Molecular Reactions and Assembly through Hydrogen-Modified Synthesis: From Triarylamine Monomer to 2D Covalent Organic Framework. *ACS Nano* **17**, 7366–7376 (2023).

39. R. Zuzak, P. Brandimarte, P. Olszowski, I. Izydorczyk, M. Markoulides, B. Such, M. Kolmer, M. Szymonski, A. Garcia-Lekue, D. Sánchez-Portal, A. Gourdon, S. Godlewski, On-Surface Synthesis of Chlorinated Narrow Graphene Nanoribbon Organometallic Hybrids. *J. Phys. Chem. Lett.* **11**, 10290-10297 (2020).

40. Y.-Y. Sung, H. Vejayan, C. J. Baddeley, N. V. Richardson, F. Grillo, and R. Schaub, Surface Confined Hydrogenation of Graphene Nanoribbons. *ACS Nano* **16**, 10281-10291 (2022).

41. C. Sánchez-Sánchez, J.I. Martínez, N. Ruiz del Arbol, P. Ruffieux, R. Fasel, M. Francisca López, P.L. de Andres, J.Á. Martín-Gago, On-Surface Hydrogen-Induced Covalent Coupling of Polycyclic Aromatic Hydrocarbons via a Superhydrogenated Intermediate. *J. Am. Chem. Soc.* **141**, 3550-3557 (2019).

42. L. Gross, F. Mohn, N. Moll, P. Liljeroth, G. Meyer, The chemical structure of a molecule resolved by atomic force microscopy. *Science* **325**, 1110−1114 (2009).

43. A. Mairena, M. Baljozovic, M. Kawecki, K. Grenader, M. Wienke, K. Martin, L. Bernard, N. Avarvari, A. Terfort, K.-H. Ernst, Ch. Wäckerlin, The fate of bromine after

temperature-induced dehydrogenation of on-surface synthesized bisheptahelicene, *Chem. Sci.* **10**, 2998-3004 (2019).

44. L. Talirz, H. Söde, S. Kawai, P. Ruffieux, E. Meyer, X. Feng, K. Müllen, R. Fasel, C. A. Pignedoli, D. Passerone, Band Gap of Atomically Precise Graphene Nanoribbons as a Function of Ribbon Length and Termination. *ChemPhysChem* **20**, 2348-2353 (2019).
45. L. Talirz, H. Söde, J. Cai, P. Ruffieux, S. Blankenburg, R. Jafaar, R. Berger, X. Feng, K. Müllen, D. Passerone, R. Fasel, C. A. Pignedoli, Termini of Bottom-Up Fabricated Graphene Nanoribbons. *J. Am. Chem. Soc.* **135**, 2060-2063 (2013).
46. M. Engelund, https://app.espeem.com, accessed Jan. 29th 2023.
47. E. Rauls, L. Hornekaer, Catalyzed routes to molecular hydrogen formation and hydrogen addition reactions on neutral polycyclic aromatic hydrocarbons under interstellar conditions, *Astrophys. J.* **679**, 531-536 (2008).
48. B. Majkusiak, J. Walczak, Theoretical Limit for the SiO_2 Thickness in Silicon MOS Devices. In: Flandre, D., Nazarov, A.N., Hemment, P.L. (eds) Science and Technology of Semiconductor-On-Insulator Structures and Devices Operating in a Harsh Environment. NATO Science Series II: Mathematics, Physics and Chemistry, vol 185. Springer, Dordrecht. https://doi.org/10.1007/1-4020-3013-4_36 (2005).
49. Y. Cao, V. Fatemi, S. Fang, K. Watanabe, T. Taniguchi, E. Kaxiras, P. Jarillo-Herrero, Unconventional superconductivity in magic-angle graphene superlattices. *Nature* **556**, 43–50 (2018).
50. H. Li, S. Li, M.H. Naik, J. Xie, X. Li, J. Wang, E. Regan, D. Wang, W. Zhao, S. Zhao, S. Kahn, K. Yumigeta, M. Blei, T. Taniguchi, K. Watanabe, S. Tongay, A. Zettl, S.G. Louie, F. Wang, M.F. Crommie, Imaging moiré flat bands in three-dimensional reconstructed WSe_2/WS_2 superlattices. *Nat. Mater.* **20**, 945–950 (2021).
51. J. Franco, J.-F. de Marneffe, A. Vandooren, Y. Kimura, L. Nyns, Z. Wu, A.-M. El-Sayed, M. Jech, D. Waldhoer, D. Claes, H. Arimura, L.-Å Ragnarsson, V. Afanas'ev, A. Stesmans, N. Horiguchi, D. Linten, T. Grasser, B. Kaczer, IEEE International Electron Devices Meeting (IEDM), San Francisco, CA, USA, 2020, pp. 31.2.1-31.2.4.
52. Y. Yue, J. Wang, Y. Zhang, Y. Song, X. Zuo, Interactions of atomic hydrogen with amorphous SiO_2. *Phys. B: Condens. Matter.* **533**, 5-11 (2018).
53. J. Voigt, M. Roy, M. Baljozović, Ch.Wäckerlin, Y. Coquerel, M. Gingras, K.-H. Ernst, Unbalanced 2D Chiral Crystallization of Pentahelicene Propellers and Their Planarization into Nanographenes. *Chem. Eur. J.* **27**, 10251–10254 (2021).
54. J. Voigt, K. Martin, E. Neziri, M. Baljozović, Ch. Wäckerlin, N. Avarvari, K.-H. Ernst, Highly Stereospecific On-Surface Dimerization into Bishelicenes: Topochemical Ullmann Coupling of Bromohelicene on Au(111). *Chem. Eur. J.* **29**, e2023001 (2023).
55. Y. Zhao, D.G. Truhlar, The M06 suite of density functionals for main group thermochemistry, thermochemical kinetics, noncovalent interactions, excited states, and transition elements: two new functionals and systematic testing of four M06-class functionals and 12 other functionals, *Theor. Chem. Acc.* **120**, 215-241 (2008).
56. R. Krishnan, J.S. Binkley, R. Seeger, J.A. Pople, Self-consistent molecular orbital methods. XX. A basis set for correlated wave functions, *J. Chem. Phys.* **72**, 650-654 (1980).

57. A. McLean, G. Chandler, Contracted Gaussian basis sets for molecular calculations. I. Second row atoms, Z= 11–18, *J. Chem. Phys.* **72**, 5639-5648 (1980).

58. M. Frisch, G. Trucks, H. Schlegel, G. Scuseria, M. Robb, J. Cheeseman, G. Scalmani, V. Barone, G. Petersson, H. Nakatsuji, Gaussian 16, Gaussian, Inc, Wallingford, CT (2016).

59. Y. Li, T. Wang, K. K. Yalamanchi, G. Kukkadapu, S. M. Sarathy, Accurate thermochemistry prediction of extensive polycyclic aromatic hydrocarbons (PAHs) and relevant radicals, *Combustion and Flame* **242**, 112159 (2022).

60. Classical and Quantum Dynamics in Condensed Phase Simulations; Berne, B. J., Ciccotti, G., Coker, D. F., Eds.; WORLD SCIENTIFIC, 1998.

61. G. Henkelman, H. Jónsson, Improved Tangent Estimate in the Nudged Elastic Band Method for Finding Minimum Energy Paths and Saddle Points. *J. Chem. Phys.* **113**, 9978–9985 (2000).

62. G. Henkelman, B.P. Uberuaga, H. Jónsson, A Climbing Image Nudged Elastic Band Method for Finding Saddle Points and Minimum Energy Paths. *J. Chem. Phys.* **113**, 9901-9904 (2000).

63. P. Giannozzi, S. Baroni, N. Bonini, M.Calandra, R.Car, C. Cavazzoni, D. Ceresoli, G. L Chiarotti, M. Cococcioni, I. Dabo, *J. Phys.: Cond. Matter.* **21**, 395502 (2009).

64. J. P. Perdew, A. Ruzsinszky, G. I. Csonka, O. A. Vydrov, G. E. Scuseria, L. A. Constantin, X. Zhou, K. Burke, *Phys. Rev. Lett.* **100**, 136406 (2008).

65. S. Grimme, *J. Comput. Chem.* **27**, 1787-1799 (2006).

66. G. Kresse, D. Joubert, *Phys. Rev. B* **59**, 1758 (1999).

67. N. F. Barrera, P. Fuentealba, F. Muñoz, T. Gómez, C. Cárdenas, Formation of H_2 on polycyclic aromatic hydrocarbons under conditions of the ISM: an abinitio molecular dynamics study, *Mon. Notices Royal Astron. Soc.* **524**, 3741-3748 (2023).

68. R. M. Ferullo, C. E. Zubieta, P. G. Belelli, Hydrogenated polycyclic aromatic hydrocarbons (HnPAHS) as catalysts for hydrogenation reactions in the interstellar medium: a quantum chemical model, *Phys. Chem. Chem. Phys.* **21**, 12012-12020 (2019).

Acknowledgments: We acknowledge Dr. Łukasz Bodek for building the vacuum transfer system.

Funding: National Science Center, Poland, 2019/35/B/ST5/02666, Ministerio de Ciencia e Innovación, Spain, MCIN/AEI/10.13039/501100011033, grants No. PID2022-140845OB-C62, PID2022-139933NB-I00, TED2021-132388B-C42, PID2019-105479RB-I00 and TED2021-129416A-I00, European Regional Development Fund; Xunta de Galicia (Centro de Investigacion de Galicia accreditation 2019–2022), grant No. ED431G2019/03

Competing interests: The hydrogen induced cyclodehydrogenation is based on a patent application "A method for producing graphene nanostructures", PCT/EP2023/060258.

Supporting Information

Materials and Methods

Supplementary Text
Figs. S1 to S9